2015-1

Dual effects of β-cyclodextrin-stabilised silver nanoparticles: enhanced biofilm inhibition and reduced cytotoxicity

Swarna Jaiswal
Technological University Dublin, swarna.jaiswal@tudublin.ie

Recommended Citation

Jaiswal,S. ,Bhattacharya, K.,McHale, P. & Duffy, B. (2015) Dual effects of β-cyclodextrin-stabilised silver nanoparticles: enhanced biofilm inhibition and reduced cytotoxicity, *J Mater Sci: Mater Med* (2015) 26:52 doi:10.1007/s10856-014-5367-1

J Mater Sci: Mater Med (2015) 26:52
DOI 10.1007/s10856-014-5367-1

Dual effects of β-cyclodextrin-stabilised silver nanoparticles: enhanced biofilm inhibition and reduced cytotoxicity

Swarna Jaiswal · Kunal Bhattacharya · Patrick McHale · Brendan Duffy

Received: 23 April 2014 / Accepted: 6 September 2014

Abstract The composition and mode of synthesis of nanoparticles (NPs) can affect interaction with bacterial and human cells differently. The present work describes the ability of β-cyclodextrin (β-CD) capped silver nanoparticles (AgNPs) to inhibit biofilm growth and reduce cytotoxicity. Biofilm formation of *Staphylococcus epidermidis* CSF 41498 was quantified by a crystal violet assay in the presence of native and capped AgNPs (Ag-10CD and Ag-20CD), and the morphology of the biofilm was observed by scanning electron microscope. The cytotoxicity of the AgNPs against HaCat cells was determined by measuring the increase in intracellular reactive oxygen species and change in mitochondrial membrane potential ($\Delta\Psi m$). Results indicated that capping AgNPs with β-CD improved their efficacy against *S. epide*rmidis CSF 41498, reduced biofilm formation and their cytotoxicity. The study concluded that β-CD is an effective capping and stabilising agent that reduces toxicity of AgNPs against the mammalian cell while enhancing their antibiofilm activity.

S. Jaiswal · P. McHale
School of Biological Sciences, Dublin Institute of Technology, Kevin Street, Dublin 8, Ireland

S. Jaiswal (✉) · B. Duffy
Centre for Research in Engineering Surface Technology (CREST), FOCAS Institute, Dublin Institute of Technology, Camden Row, Dublin 8, Ireland
e-mail: swarna.jaiswal@dit.ie

K. Bhattacharya
Nanolab Research Centre, FOCAS Institute, Dublin Institute of Technology, Dublin, Ireland

K. Bhattacharya
Institute of Environmental Medicine, Karolinska Institute, Nobels Vag 13, Stockholm, Sweden

1 Introduction

Nanoparticles (NPs) have been used for various bio-applications such as bimolecular recognition, drug delivery, imaging and fluorescence sensing [1]. However, concerns have been raised over their disposal and their subsequent environmental impact. There is increasing evidence to indicate that prolonged exposure to NPs can have adverse effects on human cells [2]. Their unique physiochemical properties (small size, high surface to volume ratio, chemical composition and surface property effects) may be significant in NP-induced toxicity particularly through causing oxidative damage to mammalian cells [3].

In the past decade the antimicrobial properties of AgNPs have generated much commercial interest due to the increase in the number and variety of antibiotic resistant microbial strains encountered in healthcare facilities. The antimicrobial activity of AgNPs is due to the silver ions (Ag^+) [4], whose efficacy is known from ancient times. AgNPs have been used as a source of Ag^+ in many commercial products, including food packaging [5], antibacterial textiles [6] and medical devices [7]. AgNPs are also known to prevent biofilm formation on environmental surfaces [8]. Biofilms are complex aggregations of microorganisms that adhere to living and non-living surfaces, protecting the bacteria from the host immune system in vivo and from biocides and disinfectants in vitro [8]. Bacteria in biofilms are more resistant to antibacterial agents than free living, planktonic bacteria due to the biofilm matrix acting as a physical diffusion barrier and to physiological differences in bacterial cells within the matrix.

The toxicity of AgNPs has been studied in different cell lines including lung epithelial (A549), ocular epithelial lung fibroblast (IMR-90), rat brain and glioblastoma

Published online: 18 January 2015

(U251) cells [9, 10]. AgNP synthesis techniques have been developed utilizing various stabilising and reducing agents along with biopolymers such as starch [11], chitosan [12], cyclodextrin (CD) [13] and sophorolipids [14]. These capping agents provide a large number of hydroxyl groups that can co-ordinate with the metal ions. Moreover, they provide a means of controlling the size, shape and dispersion of the NPs and subsequent release of the active ionic silver. Capping AgNPs with particular polymeric compounds has also been shown to modify their cytotoxicity, biocompatibility and biodegradability [15].

Cyclodextrins have been extensively utilized as pharmaceutical ingredients and food additives to enhance solubility, bioavailability and stability [16]. The physicochemical properties of β-CDs such as hydrophilicity, high molecular weight (MW), their large number of hydrogen donors and acceptors and inclusion capacities, have made them ideal capping agents for the stable delivery of AgNPs. Previously, our study showed that β-CD capped AgNPs have excellent antibacterial activity against planktonic bacteria (*Escherichia coli, Pseudomonas aeruginosa* and *Staphylococcus aureus).*

Generally, it has been observed that the concentration of antimicrobial agents which are effective against planktonic bacteria may be ineffective against those in biofilms and mammalian cells [17]. However, as per the authors knowledge, no study was carried out to evaluate the effect of β-CD capped AgNPs on the biofilm forming bacteria and mammalian cells. Therefore, the present work is focused on dose-dependent study of β-CD capped AgNPs against biofilm forming bacteria. Consequently, the effects of native and capped AgNPs on mammalian skin epithelial (HaCat) cells and their modulation by exposure to different capping concentrations of β-CD were examined. The effect of β-CD capping of AgNPs on their generation of intracellular reactive oxygen species (ROS) and their reduction of inner mitochondrial membrane potential in the HaCat cells was also analysed.

2 Materials and methods

2.1 Synthesis and characterisation of β-CD capped AgNPs

Silver nanoparticles (AgNPs) capped with different concentrations of β-CD were synthesised and characterised as described previously paper [18]. The β-CD-capped Ag NP's were synthesized by reducing silver nitrate with sodium borohydride in the presence of various concentrations (5, 10 and 20 mM) of β-CD as a capping agent. In brief, aqueous β-CD solutions of different concentrations were prepared and sonicated for 10–20 min in order to obtain the transparent solution. Equal volumes of β-CD solution were mixed with equal volume of 2 mM$AgNO_3$ with stirring for 15 min after which equal volumes of ice cold 20 mM $NaBH_4$ solutions were added. The resultant solutions were stirred for 24 h to stabilize them. The total Ag concentrations of [Ag] 2, 4, 8, 16 and 33 ppm were used for this study. A β-CD-free native AgNP was similarly prepared. All chemicals were purchased from Sigma-Aldrich (Ireland) and were used without further purification. All aqueous solutions were made using highly purified deionised water produced by a Milli-Q SP ultra pure water system.

2.2 Physicochemical characterization

UV–vis–NIR absorption spectra of the native and β-CD capped AgNPs were recorded in the 300–800 nm wavelength range using a spectrophotometer (Perkin-Elmer Lambda 900) operating at a resolution of 2 nm. The average diameter and zeta potential of the AgNPs were measured by DLS using a Malvern Zeta Sizer Nano ZS (Malvern Instruments, Worcestershire, UK). This instrument is equipped with a 4 mW He–Ne laser and measures the dynamic light (back) scattering (DLS) from a suspension at an angle of 90°. The AgNPs suspended in double distilled milliQ water and filtered by syringe filter (0.22 mm), were determined at 25 °C. The AgNPs were drop-cast onto standard Formvar-coated TEM copper grids (200–300 nm) and air dried. The morphology of all samples was then determined using a JEM-100CX II transmission electron microscope (TEM) JEOL operated at an accelerating voltage of 100 kV.

Inductively coupled plasma atomic emission spectroscopy (ICP–AES) was used to determine the silver [Ag^+] concentration (ppm) in the solution. It was carried out on the clear supernatants obtained after centrifugation at 1,400 rpm for 20 min. ICP–AES was performed using a Varian Liberty 150 instrument optimized at 328.068 nm for aqueous solutions to quantify the amounts of silver contained in the samples. A calibration curve was prepared from a 1,000 ppm standard silver solution (ARISTAR® silver, BDH, England, UK) by appropriate dilution. A new calibration curve was prepared for each set of data.

2.3 Quantification of biofilm

Biofilm quantification, using crystal violet staining (CVS), was performed (with some modifications) as previously reported [19]. Native and capped (Ag-10CD, Ag-20CD) AgNPs (250 µl) of Ag concentrations 16 and 8 ppm were pipetted into 24 wells of a microtitre plate and biofilm positive bacteria *S. epidermidis* CSF 41498 (250 µl of 1.5×106 CFU ml^{-1}) added. The plates were incubated at

37 °C for 4 days. The blank wells contained NPs without bacterial cultures and the control wells consisted of the bacterial culture alone. After incubation, the suspensions were removed and the wells gently rinsed thrice with sterile water to remove loosely associated bacteria. The biofilm formed was stained with 1 %w/v CV solution (500 µl) for 45 min and then the wells were washed thrice with sterile distilled water. Biofilms appeared as purple rings on the surfaces of the wells. The biofilms were quantified by eluting the CV with 95 % ethanol (500 µl) for 10 min and transferring aliquots (100 µl) of the eluants to wells of another microtitre plate for OD measurement at 570 nm. The absorbance values were considered to be directly proportional to the amount of biofilm formed on the surface. The results obtained were compared to the nanoparticle-free bacterial control to determine the percentage biofilm inhibition.

2.4 Characterisation of biofilm by SEM

Three clean glass slides (1 cm^2) were placed in separate small sterile petri dishes, containing 2.5 ml of (a) sterile water (control), (b) native AgNPs and (c) capped AgNPs (Ag-20CD) at [Ag] of 8 ppm and *S. epidermidis* CSF 41498 (2.5 ml, 1.5 × 106 CFU ml^{-1}) added. The dishes were incubated at 37 °C for 4 days. To assess the effect of the AgNPs on preformed biofilms bacterial culture (2.5 ml) was added to a glass slide in another sterile petri dish and incubated at 37 °C for 4 days after which Ag-20CD (2.5 ml, 8 ppm) was added and the dish incubated at 37 °C for 16 h. After incubation all slides were rinsed gently with sterile water,dried and mounted on aluminium stubs and gold coated (Cressington 208HR sputter coater) for analysis of the morphology of attached bacteria using a Hitachi SU70 scanning electron microscope (SEM) operating at 2 and 15 keV.

2.5 Toxicological analysis

2.5.1 *Cell culture*

Immortalised non-cancerous human keratinocyte cells (HaCat) were cultured in Dulbecco's modified Eagle's Medium Nutrient Mixture F-12 HAM (DMEM-F12) (Sigma-Aldrich, Ireland) supplemented with 5 % foetal bovine serum (FBS), 45 IU ml^{-1} penicillin and 45 IU ml^{-1} streptomycin at 37 °C in 5 % CO_2.

2.5.2 *Cytotoxicity assay*

For the cytotoxicity assay, HaCat cells were grown in 96 well microtitre plates for 24 h at 37 °C in 5 % CO_2, washed with phosphate buffered saline (PBS, 100 µl $well^{-1}$), and treated with native and β-CD capped AgNPs containing increasing concentrations of Ag (2–33 ppm in cell culture medium containing 5 % FBS). Two HaCat cell concentrations, 1 × 10^5 and 8 × 10^4 cells ml^{-1} $well^{-1}$, were used and the plates were incubated for 24 and 48 h respectively at 37 °C in a 5 % CO_2 humidified incubator. Cell viability was determined by the Alamar Blue (AB, Biosource, UK) assay [20]. Briefly, wells were emptied, rinsed with sterile PBS, and AB reagent (100 µl of 5 % w/w in fresh medium without supplements) added to each. *Cis* platin (*cis*-diamminedichloroplatinum (II) (Sigma Aldrich, Ireland) at a concentration of 13 µM used as the positive control [21]. After incubation for 3 h at 37 °C the AB fluorescence was measured using a microplate reader at the respective excitation and emission wavelengths of 540 and 595 nm. All the experiments were done twice in six replicates for statistical analysis.

2.5.3 *Measurement of intracellular ROS*

The generation of ROS was determined using carboxy-2′,7′-dichloro-dihydrofluorescein diacetate (carboxy H_2-DCFDA, Invitrogen, Ireland) using a standard protocol [22]. In brief, HaCat cells were seeded at a density of 1 × 10^5 cells ml^{-1} $well^{-1}$ in 96 well plates and incubated at 37 °C for 24 h. The cells were washed twice with sterile PBS (100 µl $well^{-1}$) and treated for 2, 4, 12 and 24 h with native and β-CD capped AgNPs of Ag concentrations 2–33 ppm (in cell culture medium containing 5 % FBS) at 37 °C. Cells treated with DMSO were included as negative controls and *cis*-diammineplatinum (II) dichloride (cisplatin) at a concentration of 13 µM as the positive control [23]. Following incubation, the wells were washed twice with sterile PBS (100 µl $well^{-1}$). Carboxy H2DCFDA dye was added at a concentration of 10 µM (5 µl dye mixed with 8.65 µl of concentrated DMSO and transferred into 8 ml warm PBS) at 100 µl $well^{-1}$ and the plates were incubated at 37 °C, in 5 % CO_2 for 1 h. The dye solution was removed and the cells were washed twice with PBS (100 µl $well^{-1}$). The fluorescence of the oxidized carboxy H_2DCFDA dye was measured using a microplate reader at the respective excitation and emission wavelengths of 490 and 545 nm. All the experiments were done twice in six replicates for statistical analysis. The values obtained were expressed as the percentage ROS generation with respect to the control (no AgNPs). Detection of the fluorescent form of H_2DCFDA, carboxydichlorofluorescein, indicated intracellular ROS generation. The higher the intensity of the fluorescence, the greater the ROS generated.

2.5.4 *Mitochondrial membrane potential*

The effect of β-CD capping on the permeability of AgNPs into the cell mitochondrial membrane was measured by a

fluorimetric assay using Rhodamine 123 dye [22]. For this assay, HaCat cells (1×10^5 cells ml^{-1} $well^{-1}$) were placed in a microtitre plate and incubated for 24 h. The wells were emptied, washed twice with sterile PBS (100 µl $well^{-1}$) and treated for 2, 4, 12 and 24 h at 37 °C with [Ag] of 2–33 ppm of both β-CD capped and native AgNPs suspended in cell culture medium containing 5 % FBS. As a negative control, cells were treated with normal cell culture media and cell culture media containing 11 µM of valinomycine B was used as a positive control [21]. Following incubation at 37 °C, The wells were washed with sterile PBS (100 µl $well^{-1}$), Rhodamine 123 dye (5 µM, 100 µl $well^{-1}$) was added, the plates were incubated at 37 °C in 5 % CO_2 for 30 min, the dye was removed and the cells were washed twice with PBS (100 µl $well^{-1}$). The fluorescence was measured using a microplate reader at the respective excitation and emission wavelengths of 488 and 535 nm. All the experiments were done twice for six replicates for statistical analysis. A decrease in rhodamine fluorescence intensity with respect to the control (no AgNPs) indicated a reduction in mitochondrial membrane potential.

2.6 Statistical analysis

All statistical analyses were performed using STATGRAPHICS Centurion XV. The statistical significance (95 % confidence level ($P < 0.05$)) between the means of the native and capped AgNPs was determined by ANOVA followed by multiple range tests (least significant difference). Within each concentration range groups were defined where all samples denoted as "a" were equivalent but statistically different from samples denoted by "b" and so on.

3 Results

3.1 Physicochemical characterization

$AgNO_3$ was reduced with $NaBH_4$ and capped with β-CD with different concentrations (5, 10 and 20 mM) and the UV–visible absorption spectrum of the resulting solutions were measured. The colloidal solutions of the AgNPs showed a typical surface plasmon absorption band around 400 nm (Fig. 1a). TEM micrographs of both native (Fig. 1b) and capped (Fig. 1c) AgNPs revealed particles that were nearly spherical in shape. The size of the β-CD capped AgNPs was smaller than their native AgNPs and their average size decreased with an increase in β-CD concentration. Particle size distribution analysis using a dynamic light scattering technique (DLS) showed the native AgNPs to have a hydrodynamic diameter of

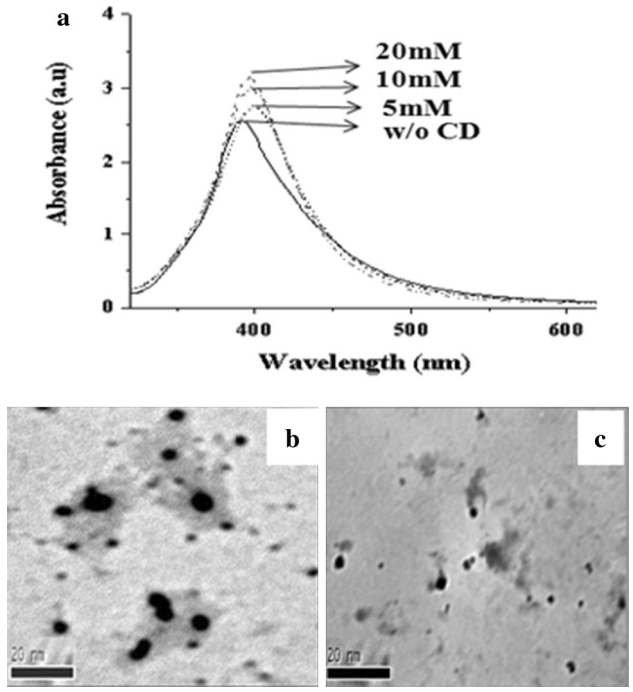

Fig. 1 **a** UV–vis absorption spectra of AgNPs native (w/o β-CD) and capped with different concentrations, 5, 10, and 20 of β-CD, **b** transmission electron microscopic images of native AgNPs and **c** Ag-20CD NPs

16 ± 2.0 nm. Capping of the AgNPs with increasing molar concentrations of β-CD (5CD 10CD and 20CD) was found to decrease their average hydrodynamic diameter respectively 6 ± 0.6 nm, 5 ± 1 d nm and 4 ± 1 nm, by reducing particle growth during synthesis. The native AgNPs had a high zeta potential (−28 ± 1.4 mV), which was reduced with the increasing molarity of β-CD capping. At the highest β-CD concentration (20 mM) the low zeta potential (−38 ± 1.3 mV) was observed where as higher zeta potential −35 ± 2.1 and −32 ± 1.6 mV were observed in the presence of Ag-10CD and Ag-5CD respectively. AgNPs were quantified (ICP–OES) by subtracting the initial [Ag^+] (from 220 to 43 ppm) measured in the supernatant after the centrifugation of β-CD capped AgNPs suspension.

3.2 Quantification of biofilm

S. epidermidis is the most common bacterium isolated from medical devices such as vascular catheters, prosthetic implants and intrauterine devices, where it often forms biofilms. The effect of native and capped AgNPs, of different Ag concentrations (8 and 16 ppm), on biofilm formation by *S. epidermidis* CSF 41498 was determined by the CVA (Fig. 2). β-CD capped AgNPs (both Ag-10CD and Ag-20CD) inhibited biofilm formation by more than

90 %, whereas native AgNPs reduced it by approximately 10–15 % (Fig. 2b).

3.3 Characterisation of biofilm by SEM

SEM images of *S. epidermidis* CSF 41498 incubated with AgNPs and Ag-20CD at an Ag concentration of 8 ppm are presented in Fig. 3. The control slide shows surface colonisation by biofilm (Fig. 3a), while treatment with AgNPs produced less biofilm (Fig. 3b). Ag-20CD inhibited the bacterial growth and thereby prevented biofilm formation (Fig. 3c). SEM images also confirmed that preformed biofilm was damaged by Ag-20CD at concentration of 8 ppm (Fig. 3d).

3.4 Cytotoxicity assay

The toxicity study demonstrated that there was no significant difference ($P > 0.05$) in cell viability in HaCat cells exposed to the control or to capped AgNPs with the increasing Ag concentrations and exposure times, whereas the percentage cell viability significantly ($P < 0.05$) decreased with exposure to native AgNPs of increasing Ag concentrations (8–33 ppm.) in comparison to the control (Fig. 4a, b). At a [Ag] of 16 ppm there was a 30 % lower viability in HaCat cells exposed to native compared to capped AgNPs. This difference increased to 63 % at a [Ag] of 33 ppm. Below 8 ppm [Ag], there was no significant difference ($P > 0.05$) in cell viability among all test samples (Fig. 4a). The cell viability decreased significantly ($P < 0.05$) from 81 to 26 % by increasing [Ag] from 4 to 33 ppm after 48 h exposure to AgNPs. There was 100 % viability of the cells exposed to β-CD capped AgNPs with no significant difference between Ag-10CD and Ag-20CD (Fig. 4b). At 33 ppm [Ag] there was a linear inverse relationship between concentration of β-CD and cytotoxicity at the two measured exposure time points (24 h $R^2 = 0.917$) and (48 h $R^2 = 0.955$).

3.5 Generation of ROS

The fluorescent dye H_2DCFDA was used to measure intracellular ROS generation after exposure of HaCat cells to AgNPs. Native AgNPs induced ROS generation as exposure time increased from 4 h to 24 h, while β-CD capped equivalents did not (Fig. 5a). There was no significant ($P > 0.05$) difference in ROS generation after 4 h of exposure of HaCat cells to native AgNPs or the control. At [Ag] of 8–33 ppm β-CD capping significantly ($P < 0.05$) reduced (by up to 30 %) ROS generation compared to the control (Fig. 5a 1). There was a slight reduction of ROS with increases in [Ag] and exposure time.

After 12 h exposure to the native AgNPs (8 ppm), the percentage ROS generated was significantly ($P < 0.05$) increased (46 %) with respect to the control. At a [Ag] of 33 ppm the increase was up to 59 %. At low [Ag], there was no significant difference between the effect of native and capped AgNPs. Capped AgNPs showed no increase in ROS generation compared to the control over the [Ag] range 8–33 ppm (Fig. 5a 2). The percentage ROS generated by HaCat cells increased from 39 to 51 % as [Ag] of native AgNPs increased from 8 to 33 ppm after 24 h exposure. A 38–42 % reduction in ROS generation was observed in the presence of Ag-20CD (Fig. 5a 3). There was no significant ($P > 0.05$) difference between Ag-10CD and Ag-20CD. This result suggests that β-CD may act as a ROS scavenger reducing the ROS generation by AgNPs in HaCat cells.

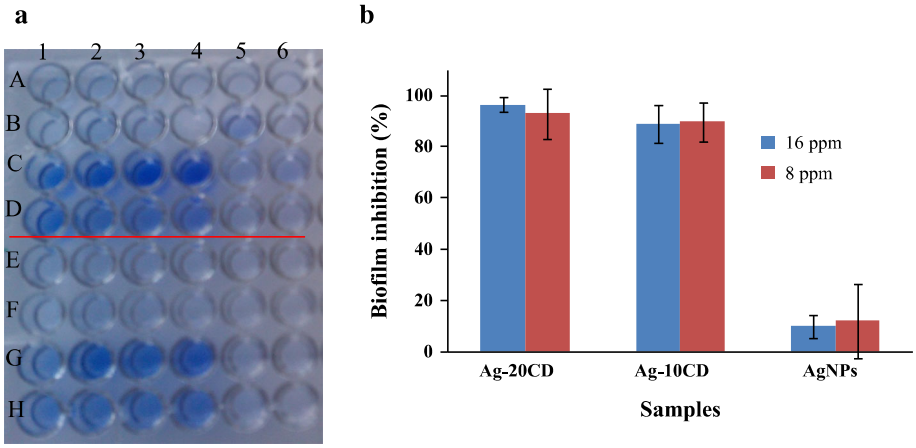

Fig. 2 Effect on biofilm formation by *S. epidermidis* CSF 41498 of native and β-CD capped AgNPs (Ag-10CD and Ag-20CD) of Ag concentrations 8 and 16 ppm. (a) crystal violet ethanol eluent in microtitre plate, where rows *A–D* are from 8 ppm Ag of (*A*) Ag-10CD, (*B*) Ag-20CD, (*C*) AgNPs and (*D*) Control; *rows E–H* are from 16 ppm of same samples; *columns 5*, *6* are from blanks containing NPs without bacteria and rows D1–4 and rows H1–4 are from controls containing only bacteria (10^6 CFU ml^{-1}). **b** *Graph* showing percentage biofilm inhibition of treated bacterial suspensions when compared to the untreated control

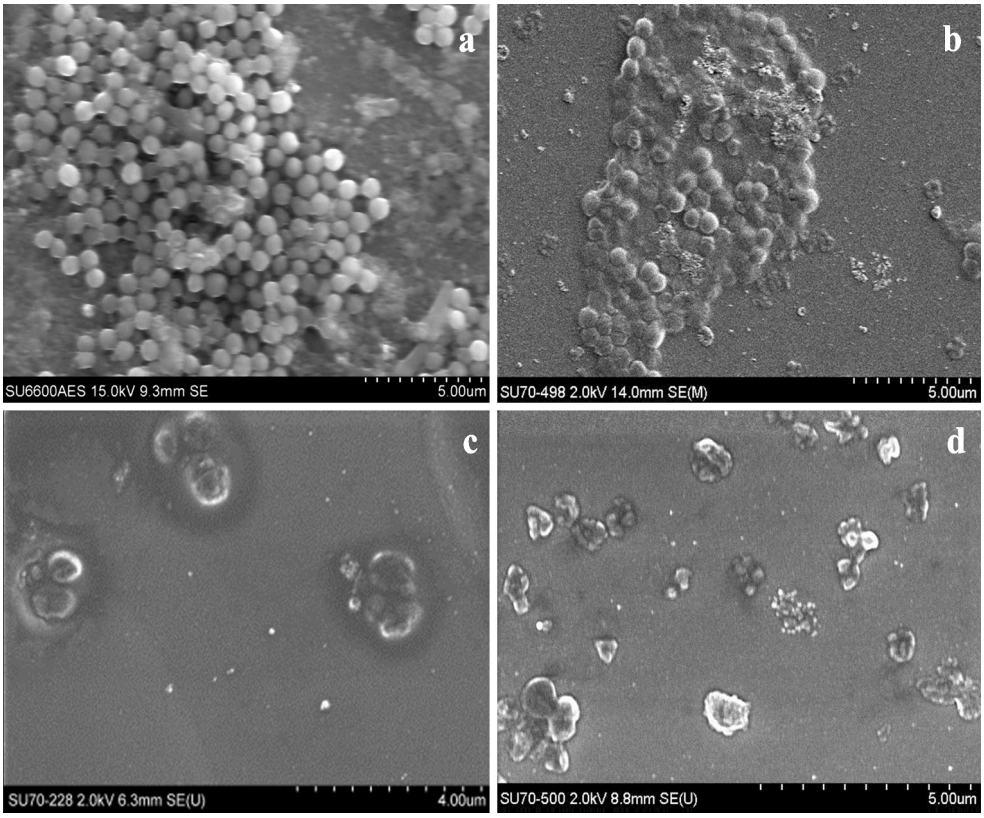

Fig. 3 *S. epidermidis* CSF CSF 41498 forming (**a**) biofilm in the absence of AgNPs (control), (**b**) some damaged biofilm in the presence of AgNPs, and (**c**) no biofilm in the presence of Ag-20CD at 8 ppm of Ag. **d** Preformed biofilm disrupted in the presence of Ag-20CD at 8 ppm

3.6 Mitochondrial membrane permeability

In order to find the mitochondrial membrane permeability of the cells in the presence of β-CD capped AgNPs and native AgNPs, fluorimetric assays were performed using Rhodamine 123 dye. After 4 h exposure of HaCat cells to native AgNPs (4 ppm), an approximate 37 % reduction in fluorescence was observed with respect to the control and 33 % compared to Ag-20CD (Fig. 5b 1). The fluorescent intensity significantly ($P < 0.05$) decreased with the increasing exposure time (4–24 h) to native AgNPs while no significant ($P > 0.05$) reduction in fluorescence was observed when cells were exposed to capped AgNPs (Fig. 5b 1–3). There was no significant ($P > 0.05$) difference between the effect of Ag-10CD and Ag-20CD on mitochondrial membrane potential.

4 Discussion

Biofilm proliferation remains a major cause of death and disability for many susceptible people across the world. Microorganisms can adapt various strategies to respond to antibacterial agents and maintain the impact of infection site disease. Therefore it is vitally important to design more effective therapeutic agents to overcome these challenges. In recent times, metal based nanoparticles have received a lot of attention as therapeutic agents because of their wide range of bioactivities and specific mode of action. Among the various metals, silver ions or salts are known for their potent antibacterial activity. However, they have only limited use as therapeutic agents because of their high toxicity to human cells and low chemical stability. In this study, stable silver nanoparticles were prepared in the presence of β-CD as a capping agent. Critically, results showed that a specific dose of β-CD capped AgNPs can protect the formation of biofilms as well as reduced the cytotoxicity towards mammalian cells.

In order to understand the characteristics of the synthesised β-CD capped AgNPs UV–vis spectra were recorded. Results showed a single narrow peak at around 400 nm; known to characteristic of the surface plasmon resonance (SPR) absorption band, occurring due to the collective oscillation of electrons of AgNPs in resonance with the light wave. The use of β-CD as a capping agent resulted in a hypochromic red shift of up to 10 nm [1].

The absorbance intensity of the solutions increased with β-CD concentration. Since the intensity of the plasmon

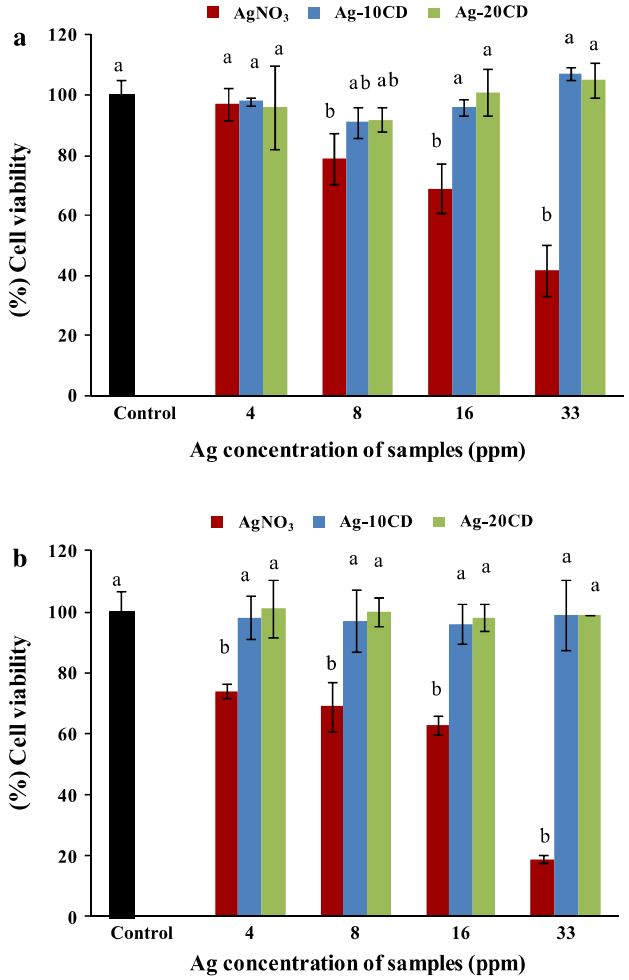

Fig. 4 Percentage viability of human keratinocytes (HaCat) exposed for **a** 24 and **b** 48 h to different concentrations of native and capped (Ag-10CD and Ag-20CD) AgNPs. *Asterisk* within each concentration, significantly ($p < 0.05$) different values are labelled by *different letter* 'a-d'. Values not significantly different are labelled with the *same letter*

resonance depends on the shape, cluster size, the metal and its surrounding environment, the number of particles cannot be related linearly to the absorbance intensities. Absorption spectra of the pale yellow capped AgNPs and native AgNPs indicated the presence of roughly spherical AgNPs which has also confirmed by TEM result. However, the shape of the plasmon bands indicated a small variation in the particle size. TEM image (Fig. 1c) shows that the nanoparticles obtained by using a 20 mM concentration of β-CD spherical in shape, smaller in size and well dispersed. The average size of the particles decreases as the concentration of β-CD was increased from 5 to 20 ppm. The growth of particles was suppressed drastically due to relative concentration of β-CD molecules.

The zeta potential is an important index which reflects the intensity of repulsive forces between particles and the stability of the dispersion and is routinely used to predict the relative stability of aqueous colloidal samples [23]. If the zeta potential is >30 or <−30 mv, the particles tend to repel each other, which increases the dispersion stability. As the zeta potential moves towards 0 mv (the isoelectric point), the possibility of particle aggregation increases, leading to a reduced suspension stability. The result indicated a relatively stable colloidal suspension at the highest β-CD concentration; suggesting that β-CD improves the AgNPs physiochemical properties such as solubility and stability. In solid or solution state, β-CD forms a cone-shaped molecule with the hydroxyl groups on the outside of the molecule, providing a hydrophilic outside and a hydrophobic cavity [24]. Ag^+ and AgNPs can both occur in solution so it is important to find the concentration of Ag^+ and their transformation into AgNPs in the β-CD capped systems. Based on ICP-AES results it was determined that about 80 % of the Ag^+ formed AgNPs.

There are numerous recent publications related to the β-CD capped silver nanoparticles which exhibit different characteristics and applications to native AgNPs. Researchers prepared AgNPs using the aminated β-CD as a reducing and stabilizing agent and showed the appearance of a plasmon peak around 400 nm indicates the formation of spherical particles [25]. Other authors synthesised AgNPs using an aqueous silver nitrate solution in the presence of glucose as a reducing agent, sodium hydroxide as a reaction catalyst and β-CD as a stabilizer [13]. The result indicated the formation of pseudo-spherical larger nanoparticles an average of 28 nm diameter. The investigation also showed that the antibacterial activity of synthesized β-CD-coated silver nanoparticles against the microorganism *Escherichia coli*. There was an research which showed the delay in bacterial growth (*E. coli* ATCC 11229, *P. aeruginosa* ATCC 27852 and *S. aureus* ATCC 25923) in the presence of β-CD-capped silver nanoparticles compared to their uncapped equivalents [18]. The synthesies of silver nanoparticles were carried out by using $NaBH_4$ as a reducing agent and β-CD as a capping agent.

The synthesized 10 mM and 20 mM β-CD capped AgNPs were performed against biofilm forming bacteria *S. epidermidis* (Figs. 2, 3). The quantitative and qualitative results exhibited the β-CD-AgNPs concentration dependent inhibition of biofilm colonization on the surface. The Ag concentration 8 and 16 ppm of β-CD capped AgNPs (Ag-10CD and Ag-20CD) inhibited the biofilm formation, however, native AgNPs were unable to damage the biofilm at the dose of 8 and 16 ppm. There is evidence in the literature, showing that antibiofilm efficacy of gum arabic capped silver nanoparticles (GA-AgNPs) were concentration dependent. The treatment of catheters with GA-AgNPs 50 $\mu g ml^{-1}$ has resulted in 95 % inhibition of bacterial colonization (*P. aeruginosa)* [26].

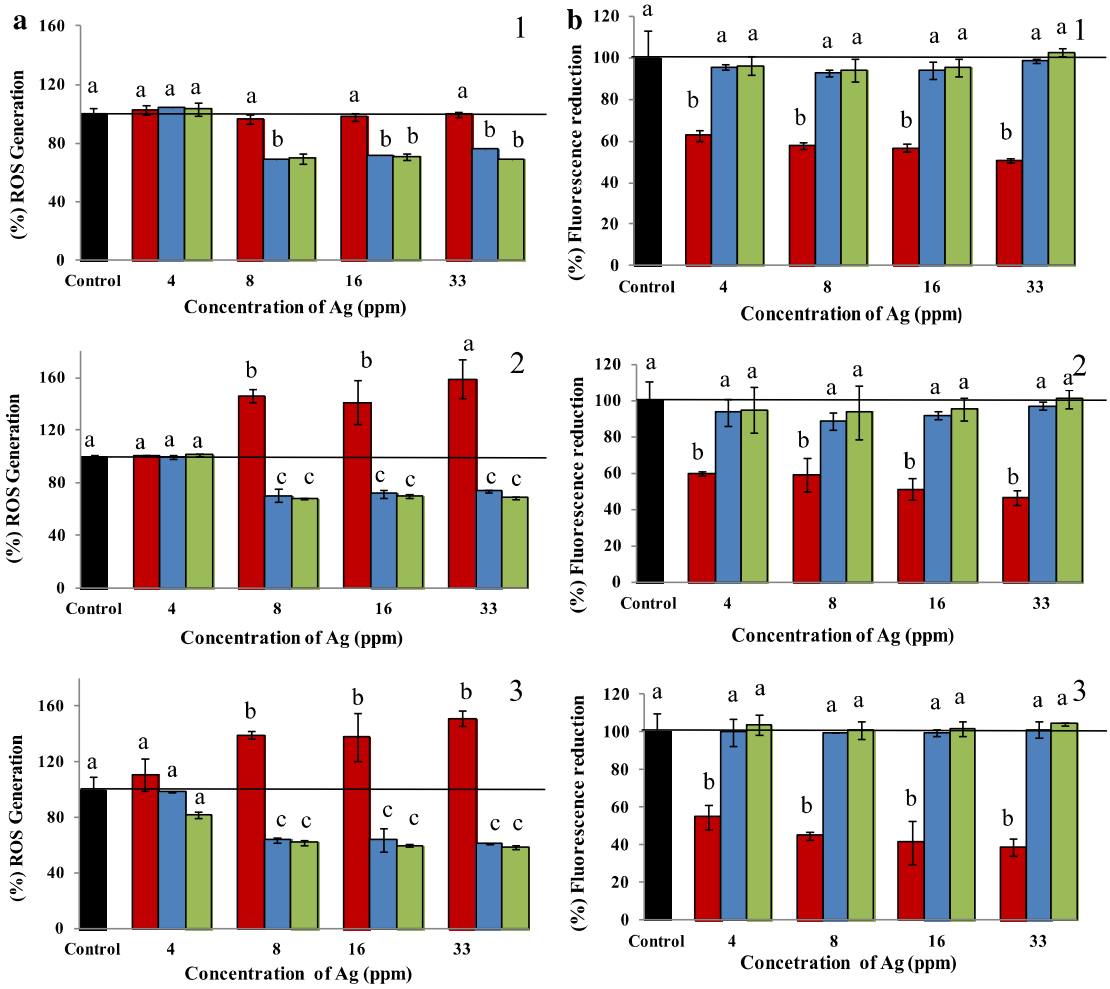

Fig. 5 **a** Effect of native AgNPs (*red*), Ag-10CD (*blue*) and Ag-20CD (*green*) on the generation of ROS in human keratinocytes (HaCat) exposed for (1) 4 h, (2) 12 h and (3) 24 h. The % ROS generation of the control cells (*black*) was considered 100 %. 5. **b** Mitochondrial membrane potential, ΔΨm, (% fluorescence) measurement in human keratinocyte (HaCat) cells exposed to different Ag concentrations of native AgNPs (*red*), Ag-10CD (*blue*) and Ag-20CD (*green*) for exposure time periods of (1) 4 h, (2) 12 h and (3) 24 h. The % fluorescence of the control cells (*black*) was considered 100 %. *Asterisk* within each concentration, significantly ($p < 0.05$) different values are labelled by *different letter* 'a-d'. Values not significantly different are labelled with the *same letter* (Color figure online)

Further, antibiofilm properties of capped AgNPs were validated by the SEM analysis. The control slide shows surface colonisation by biofilm (Fig. 3a), while treatment with AgNPs produced fewer biofilm with evidence of damage to the cocci (Fig. 3b). Ag-20CD at 8 ppm inhibited the bacterial growth and thereby prevented biofilm formation (Fig. 3c). Moreover, the results indicate that β-CD capped AgNPs not only impede the formation of biofilm as well as disrupted the preformed biofilm in the presence of Ag-20CD at 8 ppm. In the presence of capped AgNPs, the modulation of biofilm formation may be due to lower particle aggregation along with fast particle diffusion through the biofilm channels. AgNPs have been reported to impair exopolysaccharide synthesis in *P. aeruginosa* and *S. epidermidis* and, in consequence, limit biofilm formation [27].

Cell viability assays give information on metabolic activities, cell survival and death. AgNPs have been shown to induce toxicity in cells derived from a variety of organs. These differences were largely attributed to individual AgNP preparation methodologies and target cells. Dose dependent cytotoxicity responses from the Alamar blue assay indicated that native AgNPs had a toxic effect on the basic cellular metabolism and proliferation of the cells (Fig. 4). The observed decrease in the reduction of the Alamar blue dye indicates resistance of resazurin oxidation to resorufin. This redox reaction could not happen as cytosolic and mitochondrial oxidoreductase enzyme activities were

decreasing with increasing [Ag]. Capping of AgNPs with β-CD had a protective effect which reduced their cytotoxicity.

Other studies have shown that AgNPs that did not contain any surface modifiers or stabilisers had a significant cytotoxic effect on HaCat [20] and human liver cells [28]. Equivalent starch-capped AgNPs had no effect on cancer cell lines U251, fibroblasts IMR-90 or on the mouse macrophage cell line RAW264 because of the slower release of Ag^+ [11]. In contrast chitosen coated AgNPs were also observed to exhibit no apparent cytotoxic effect on macrophages [29]. The toxicity of AgNPs has been attributed to the release of Ag^+ as a result of their interaction with oxygen and protons in the medium.

Mitochondria are found in eukaryotic cells and are crucial for several cell functions. The mitochondrial inner membrane is negatively charged due to rich level of glycoproteins. Consequently, a large number of protons are attracted by the inner membrane inducing a transmembrane potential. The inner mitochondrial membrane potential plays an important role in maintaining polarity and normal electron transport chain functionality. Mitochondrial membrane potential can be monitored by the fluorescent dye, R123, which is an aromatic, lipophilic, cell permeable cationic fluorescent dye that preferentially enters into mitochondria based on their highly negative membrane potential. When mitochondrial membrane potential decreases due to cell damage, the concentration of the dye in the mitochondria decreases as does R123 fluorescence [30]. The results (Fig. 5b) indicate that β-CD has the capacity to protect the cell from mitochondrial membrane damage.

In the cytotoxicity assays, mitochondrial membrane potential destruction in cells following exposure to AgNPs leading to ROS overproduction and resulting in oxidative stress has been implicated as a major cause of toxicity [28]. The ROS study shows (Fig. 5a) significant reduction in ROS generation by HaCat cells at [Ag] 8–33 ppm after 4 h exposure to capped AgNPs compared with control cells. It has been previously reported that AgNPs (33 ppm after 5 h) can induce a high level of cellular oxidative stress in HaCat cells [20]. The present study indicates that oxidative stress can be directly related to the [Ag] and the exposure times.

AgNPs have been found to cause a reduction in glutathione (GSH) levels and an elevation in ROS levels trigger many cellular pathways, including cytokine activation and caspase activation [31], which can lead to cellular death. They can also damage the nuclear DNA by altering the chemical structure of the nucleotide bases and the deoxyribosyl backbone.

Exposure of HaCat cells to β-CD capped AgNPs caused no significant change in mitochondrial membrane potential and seemed to cause a decrease in ROS compared to the control. The ability of β-CD to quench ROS radicals could enable the AgNPs to act against a number of free radicals. Importantly, these results indicate that β-CD capped AgNPs have no cytotoxic effect on HaCat cells while simultaneously improving antibiofilm capabilities. Increasing the β-CD concentration reduced the cytotoxicity of the AgNPs. However, this mechanism has not been fully investigated in the context of other apoptosis pathways.

5 Conclusion

In summary, the study demonstrated that the capping agent β-CD reduced the size of AgNPs and changed their physiochemical properties. The dual effect of β-CD capping was demonstrated to increase the antibiofilm properties of the AgNPs and reduce their cytotoxic effects on HaCat cells at the Ag bactericidal concentration. Native AgNPs increased ROS generation and decreased mitochondrial membrane potential in the HaCat calls whereas capped AgNPs reduced the oxidative stress by reducing ROS and leaving the mitochondrial membrane potential unchanged. Therefore, β-CD capped AgNPs have the potential to be used to produce biomaterials that resist bacterial colonisation and biofilm formation and have low toxicity to human cells.

Acknowledgments The authors would like to gratefully acknowledge Ms. Ashley Allen and Ms. Anne Shanahan for their technical assistance and Dublin Institute of Technology (Dublin, Ireland) for funding under the ABBEST scholarship and Fiosraigh research scholarship program.

References

1. Abbasi E, Milani M, Fekri Aval S, Kouhi M, Akbarzadeh A, Tayefi Nasrabadi H, Nikasa P, Joo SW, Hanifehpour Y, Nejati-Koshki K. Silver nanoparticles: synthesis methods, bio-applications and properties. Crit Rev Microbiol. 2004;0:1–8.
2. Maynard AD, Kuempel ED. Airborne nanostructured particles and occupational health. J Nanopart Res. 2005;7(6):587–614.
3. AshaRani P, Low Kah Mun G, Hande MP, Valiyaveettil S. Cytotoxicity and genotoxicity of silver nanoparticles in human cells. ACS Nano. 2008;3(2):279–90.
4. Choi O, Yu C-P, Esteban Fernández G, Hu Z. Interactions of nanosilver with *Escherichia coli* cells in planktonic and biofilm cultures. Water Res. 2010;44(20):6095–103.
5. Rhim J-W, Park H-M, Ha C-S. Bio-nanocomposites for food packaging applications. Prog Polym Sci. 2013;38(10):1629–52.
6. Hebeish A, El-Naggar M, Fouda MM, Ramadan M, Al-Deyab SS, El-Rafie M. Highly effective antibacterial textiles containing green synthesized silver nanoparticles. Carbohydr Polym. 2011;86(2):936–40.
7. Maillard J-Y, Hartemann P. Silver as an antimicrobial: facts and gaps in knowledge. Crit Rev Microbiol. 2013;39(4):373–83.
8. Stobie N, Duffy B, McCormack DE, Colreavy J, Hidalgo M, McHale P, Hinder SJ. Prevention of *Staphylococcus epidermidis* biofilm formation using a low-temperature processed silver-

doped phenyltriethoxysilane sol-gel coating. Biomaterials. 2008;29(8):963–9.
9. Chairuangkitti P, Lawanprasert S, Roytrakul S, Aueviriyavit S, Phummiratch D, Kulthong K, Chanvorachote P, Maniratanachote R. Silver nanoparticles induce toxicity in A549 cells via ROS-dependent and ROS-independent pathways. Toxicol In Vitro. 2013;27(1):330–8.
10. Grosse S, Evje L, Syversen T. Silver nanoparticle-induced cytotoxicity in rat brain endothelial cell culture. Toxicol In Vitro. 2013;27(1):305–13.
11. Mohanty S, Mishra S, Jena P, Jacob B, Sarkar B, Sonawane A. An investigation on the antibacterial, cytotoxic, and antibiofilm efficacy of starch-stabilized silver nanoparticles. Nanomed: Nanotech Biol Med. 2012;8(6):916–24.
12. Abdelgawad AM, Hudson SM, Rojas OJ. Antimicrobial wound dressing nanofiber mats from multicomponent (chitosan/silver-NPs/polyvinyl alcohol) systems. Carbohydr Polym. 2014;100:166–78.
13. Andrade PF, de Faria AF, da Silva DS, Bonacin JA, Gonçalves MDC. Structural and morphological investigations of β-cyclodextrin-coated silver nanoparticles. Colloids Surf B Biointerfaces. 2014;118:289–97.
14. Singh S, Patel P, Jaiswal S, Prabhune A, Ramana C, Prasad B. A direct method for the preparation of glycolipid–metal nanoparticle conjugates: sophorolipids as reducing and capping agents for the synthesis of water re-dispersible silver nanoparticles and their antibacterial activity. New J Chem. 2009;33(3):646–52.
15. Suresh AK, Pelletier DA, Wang W, Morrell-Falvey JL, Gu B, Doktycz MJ. Cytotoxicity induced by engineered silver nanocrystallites is dependent on surface coatings and cell types. Langmuir. 2012;28(5):2727–35.
16. Loftsson T, Brewster ME. Cyclodextrins as functional excipients: methods to enhance complexation efficiency. J Pharm Sci. 2012;101(9):3019–32.
17. Bazaka K, Jacob MV, Crawford RJ, Ivanova EP. Efficient surface modification of biomaterial to prevent biofilm formation and the attachment of microorganisms. Appl Microbiol Biotechnol. 2012;95(2):299–311.
18. Jaiswal S, Duffy B, Jaiswal AK, Stobie N, McHale P. Enhancement of the antibacterial properties of silver nanoparticles using β-cyclodextrin as a capping agent. Int J Antimicrob Ag. 2010;36(3):280–3.
19. Erriu M, Genta G, Tuveri E, Orrù G, Barbato G, Levi R. Microtiter spectrophotometric biofilm production assay analyzed with metrological methods and uncertainty evaluation. Measurement. 2012;45(5):1083–8.
20. Mukherjee SG, O'Claonadh N, Casey A, Chambers G. Comparative in vitro cytotoxicity study of silver nanoparticle on two mammalian cell lines. Toxicol In Vitro. 2012;26(2):238–51.
21. Rosado-Berrios CA, Vélez C, Zayas B. Mitochondrial permeability and toxicity of diethylhexyl and monoethylhexyl phthalates on TK6 human lymphoblasts cells. Toxicol In Vitro. 2011;25(8):2010–6.
22. Bhattacharya K, Naha PC, Naydenova I, Mintova S, Byrne HJ. Reactive oxygen species mediated DNA damage in human lung alveolar epithelial (A549) cells from exposure to non-cytotoxic MFI-type zeolite nanoparticles. Toxicol Lett. 2012;215(3):151–60.
23. Liao D, Wu G, Liao B. Zeta potential of shape-controlled TiO_2 nanoparticles with surfactants. Colloids Surf A: Physicochem Eng Asp. 2009;348(1):270–5.
24. Hebeish A, El-Shafei A, Sharaf S, Zaghloul S. Novel precursors for green synthesis and application of silver nanoparticles in the realm of cotton finishing. Carbohydr Polym. 2011;84(1):605–13.
25. Abou-Okeil A, Amr A, Abdel-Mohdy F. Investigation of silver nanoparticles synthesis using aminated β-cyclodextrin. Carbohydr Polym. 2012;89(1):1–6.
26. Ansari MA, Khan HM, Khan AA, Cameotra SS, Saquib Q, Musarrat J. Gum arabic capped-silver nanoparticles inhibit biofilm formation by multi-drug resistant strains of *Pseudomonas aeruginosa*. J Basic Microbiol. 2014;54:688–99.
27. Kalishwaralal K, BarathManiKanth S, Pandian SRK, Deepak V, Gurunathan S. Silver nanoparticles impede the biofilm formation by *Pseudomonas aeruginosa* and *Staphylococcus epidermidis*. Colloids Surf B: Biointerfaces. 2010;79(2):340–4.
28. Piao MJ, Kang KA, Lee IK, Kim HS, Kim S, Choi JY, Choi J, Hyun JW. Silver nanoparticles induce oxidative cell damage in human liver cells through inhibition of reduced glutathione and induction of mitochondria-involved apoptosis. Toxicol Lett. 2011;201(1):92–100.
29. Wei D, Sun W, Qian W, Ye Y, Ma X. The synthesis of chitosan-based silver nanoparticles and their antibacterial activity. Carbohydr Res. 2009;344(17):2375–82.
30. Solaini G, Sgarbi G, Lenaz G, Baracca A. Evaluating mitochondrial membrane potential in cells. Biosci Rep. 2007;27:11–21.
31. Li P-W, Kuo T-H, Chang J-H, Yeh J-M, Chan W-H. Induction of cytotoxicity and apoptosis in mouse blastocysts by silver nanoparticles. Toxicol Lett. 2010;197(2):82–7.